# Magnetoelastic properties of $R$Zn equiatomic compounds

P. Morin, J. Rouchy, and E. du Tremolet de Lacheisserie
*Laboratoire Louis Néel, Centre National de la Recherche Scientifique, 166X, 38042 Grenoble Cedex, France*
(Received 1 March 1977)

The magnetoelastic properties of the ferromagnetic cubic compounds of heavy rare earths with zinc ($R$Zn) are investigated. Lattice distortions occuring below the ordering point are particularly strong when tetragonal: For instance, DyZn exhibits at low temperature a spontaneous tetragonal strain expressed as $c/a - 1 = +8.1 \times 10^{-3}$. All of these magnetoelastic properties are chiefly due to the crystalline electric field splitting of the ground-state $J$ multiplet. But the tetragonal distortion observed in GdZn below the ordering point reveals pseudodipolar magnetoelastic effects to be important also; this contribution is taken into account for all the compounds. From our strain gauges and capacitance dilatometer experiments we deduce the one-ion and two-ion magnetoelastic coefficients across the series. The former ones are compared with determinations from ultrasonic measurements and their variation through the series is interpreted in terms of crystal-field theory. Finally, an attempt was made to connect these coefficients to the present knowledge of the conduction band in these CsCl-type intermetallic compounds.

## I. INTRODUCTION

The equiatomic compounds of the rare earths with zinc crystallize with the cubic CsCl-type structure.[1] This simple structure enables one to study the different interactions of $4f$ shell in a metallic surrounding in an entire series. Various experiments have been undertaken on single crystals of these $R$Zn compounds: magnetization,[2] specific heat,[3] inelastic neutron scattering,[4] and all have shown the important effect of the crystalline electric field (CEF). But use of only a cubic CEF Hamiltonian in addition to the Heisenberg exchange term was found insufficient to perfectly describe the observed physical properties. This failure is a result of neglecting magnetoelastic effects which have been shown to be strong by a preliminary dilatometric experiment.[5]

The purpose of this paper is to present a detailed analysis of the magnetoelastic properties observed in the presence of strong CEF effects in the heavy-rare-earth compounds $R$Zn. This series is favorable for such a study: from gadolinium to thulium, the compounds are ferromagnetic and exhibit high Curie points (Table I). In addition to the anisotropy of energy, a main CEF effect consists of an anisotropic reduction of the moment as in the case of ErZn and HoZn, where the saturation can be reached under field along the different principal crystallographic axes.

In HoZn and TbZn, entropy effects due to the anisotropic splitting by the exchange field of the paramagnetic CEF level scheme lead to a thermal change of the easy direction.[3] From the various experimental results the cubic fourth- and sixth-order CEF parameters have been determined. Both $A_4\langle r^4\rangle$ and $A_6\langle r^6\rangle$ are negative in all the $R$Zn intermetallics. But their variation through the series remains far from any point-charge estimates, that is somewhat analogous to the case of rare earths in Ag and Au,[6,7] Y, and Sc.[8] As discussed elsewhere,[4] the major contribution to CEF parameters arises from the $d$ character of the conduction band on the $4f$ site. By augmented-plane-

TABLE I. Main magnetic properties in ferromagnetic $R$Zn compounds.

| $R$Zn | $T_c$ (K) | Easy axis | Saturation moment at 4.2 K [001] | [101] | [111] | $A_4\langle r^4\rangle$ (K/atom) | $A_6\langle r^6\rangle$ (K/atom) |
|---|---|---|---|---|---|---|---|
| GdZn | 270 | | | 7.30 | | | |
| TbZn | 204 | $\frac{63\ T}{[101]\ [001]}$ | | 8.85 | | $-41\pm5$ | $-83\pm10$ |
| DyZn | 140 | [001] | 9.05 | | | $-30\pm15$ | $-35\pm15$ |
| HoZn | 74 | $\frac{23\ T}{[101]\ [111]}$ | | 8.45 | 8.15 | −14 | −18 |
| ErZn | 20 | [001] | 6.81 | 6.37 | 6.44 | −36 | −18 |

wave(APW) calculations,[9] the $d$ band is found close to the Fermi level with only the $e_g$ subband occupied. This interaction between the $4f$ shell and the conduction band may be decomposed into direct and exchange Coulombic terms, and the variation of CEF parameters across a series can originate from an exchange process between the $4f$ shell and the conduction band for each rare-earth ion.

We shall discuss in Sec. II the relevant Hamiltonian of the $R$Zn problem, and derive the anisotropic magnetostrictive strains. Experimental methods are described in Sec. III. Then, we give in Sec. IV the results for each compound, beginning with GdZn. Section V is devoted to volume strains. Finally, we disuss the results.

## II. THEORY AND CALCULATION METHODS

As a first approximation, the magnetic properties of cubic $R$Zn compounds can be described in the molecular-field (MF) approximation, by the following basic Hamiltonian, expressed in fourfold axes (K/atom):

$$\mathcal{H} = W\left(x\,\frac{O_4}{F_4} + (1-|x|)\frac{O_6}{F_6}\right) - g\mu_B(\vec{H}_{ex}+\vec{H}_i)\cdot\vec{J}\,, \qquad (1)$$

where $O_4$ and $O_6$ are the Stevens-operator equivalents, the expressions for which are different along the various crystallographic axes,[10] $W$ is the scaling factor of the crystalline field, and $x$ is a measure of the ratio of fourth- and sixth-order terms. $\vec{H}_i$ is the internal field. The exchange energy $-g\mu_B\vec{H}_{ex}\cdot\vec{J}$ is written

$$[3\Theta_p/J(J+1)](\langle J_x\rangle J_x+\langle J_y\rangle J_y+\langle J_z\rangle J_z)\,,$$

where $\Theta_p$ is the experimental paramagnetic Curie temperature. Our self-consistent calculation starts with the diagonalization of the whole Hamiltonian in fourfold axes for any direction of the moment in the space, taking into account its three components. We calculate from the level scheme the partition function and the moment $\vec{M}$ as different thermodynamic functions using Maxwell-Boltzmann statistics. It is then possible to calculate the magnetization curve for any internal field direction, describing both the wavefunction purification under field and the rotation mechanism of the moment from the easy direction.

In this Hamiltonian, only the $W$ and $x$ parameters are unknown. But in favorable cases, neutron spectroscopy allows their direct determination in the paramagnetic state, without any exchange contribution. As in ErZn and HoZn,[4] the magnetic properties are well described with the same level scheme in both paramagnetic and ordered states, we are led to think that the variation of the CEF parameters due to a modification of the band structure at the ordering point is negligible in our compounds.

However, the fits of the magnetization curves may be improved, chiefly during the rotation process, if one takes into account the quadrupolar exchange via conduction electrons between magnetic ions. Treated in the MF approximation, the quadrupolar coupling is written

$$\mathcal{H}_{qq} = -K_1(\langle O_2^0\rangle O_2^0 + 3\langle O_2^2\rangle O_2^2) - 4K_2(\langle P_{xy}\rangle P_{xy}+\cdots)\,, \qquad (2)$$

where $O_2^0$, $O_2^2$, and $P_{ij}$ are the second-order Stevens operators

$$O_2^0 = 2J_z^2 - (J_x^2+J_y^2)\,, \qquad (3)$$

$$O_2^2 = J_x^2 - J_y^2\,, \qquad (4)$$

$$P_{ij} = \tfrac{1}{2}(J_iJ_j+J_jJ_i), \quad \text{with } i,j = x,y,z\,. \qquad (5)$$

In the case of weak magnetic interactions, quadrupole coupling can lead to a quadrupole ordering point, with a structural transition. Equation (2) has successfully contributed in the past to explain a great number of CEF effects, mainly on elastic constants.[11-14]

Due to the important magnetoelastic properties observed in the $R$Zn compounds, we have to complete the Hamiltonian with a magnetoelastic term $\mathcal{H}_{me}$ and the elastic energy $E_e$. Both terms are expressed as a function of the normal modes of deformation for cubic symmetry, taking into account only the terms linear with the deformations. The one-ion contribution to $\mathcal{H}_{me}$ is

$$\mathcal{H}_{me}^{I} = -B_1\left|\,\epsilon_3 O_2^0 + \sqrt{3}\,\epsilon_2 O_2^2\right| - B_2\left|\,\epsilon_{xy}P_{xy}+\cdots\right|\,, \qquad (6)$$

and the elastic energy is

$$E_e = \tfrac{1}{2}C_{B_0}(\epsilon_v)^2 + \tfrac{1}{2}(C_{11}-C_{12})_o(\epsilon_3^2+\epsilon_2^2) + 2C_{44_o}(\epsilon_{xy}^2+\cdots)\,, \qquad (7)$$

where the symmetrized strains are defined as

$$\epsilon_v = \epsilon_{xx}+\epsilon_{yy}+\epsilon_{zz}\,, \qquad (8)$$

$$\epsilon_3 = (1/\sqrt{6})(2\epsilon_{zz}-\epsilon_{xx}-\epsilon_{yy})\,, \qquad (9)$$

$$\epsilon_2 = (1/\sqrt{2})(\epsilon_{xx}-\epsilon_{yy})\,, \qquad (10)$$

and the $\epsilon_{ij}$'s are the tensor components of the strain. Note that the pure tetragonal spontaneous deformation $c/a-1$ is expressed as $\sqrt{\frac{3}{2}}\,\epsilon_3$. The $C_{ij_o}$'s are the background elastic constants without interaction, expressed in $K$/atom and $C_B = \frac{1}{3}(C_{11}+2C_{12})$ is the bulk modulus. The $B_i$'s are proportional to the magnetoelastic coefficients $B^{\Gamma}$ of Callen and Callen,[15] and are taken as constant with temperature. We neglect here higher-order contributions, as justified by Lüthi *et al.*[16] in calculations on $R$Sb magnetoelastic properties.

Furthermore, in the case of a $S$-state ion, the different $B_i$'s are null and no CEF effects are expected. But the magnetostrictive tetragonal distortion observed in GdZn compels us to also take into account the two-ions contribution to the magnetoelastic Hamiltonian $\mathcal{H}_{me}^{II}$. We shall limit $\mathcal{H}_{me}^{II}$ to the pseudodipolar (PSD) terms written in the MF model

$$\mathcal{H}_{PSD} = -D_1[\epsilon_3\{2\langle J_z\rangle J_z - (\langle J_x\rangle J_x + \langle J_y\rangle J_y)\} + \sqrt{3}\epsilon_2(\langle J_x\rangle J_x - \langle J_y\rangle J_y)] - D_2\left(\epsilon_{xy}\frac{\langle J_x\rangle J_y + \langle J_y\rangle J_x}{2} + \cdots\right). \quad (11)$$

At this point, we do not include the exchange striction, which will be treated in Sec. V.

The treatment previously described for $\mathcal{H}$ [Eq. (1)] is now applied to the whole Hamiltonian. The minimization of the free energy with respect to each strain component leads to the equilibrium value of this strain available for any direction of the moment

$$\epsilon_3 = \frac{B_1}{(C_{11}-C_{12})_o}\langle O_2^0\rangle + \frac{D_1}{(C_{11}-C_{12})_o} \times [2\langle J_z\rangle^2 - (\langle J_x\rangle^2 + \langle J_y\rangle^2)], \quad (12)$$

$$\epsilon_2 = \frac{B_1\sqrt{3}}{(C_{11}-C_{12})_o}\langle O_2^2\rangle + \frac{D_1\sqrt{3}}{(C_{11}-C_{12})_o}(\langle J_x\rangle^2 - \langle J_y\rangle^2), \quad (13)$$

$$\epsilon_{ij} = \frac{B_2}{4C_{44_o}}\langle P_{ij}\rangle + \frac{D_2}{4C_{44_o}}\langle J_i\rangle\langle J_j\rangle. \quad (14)$$

Finally, the magnetostrictive change of length can be expressed as

$$\lambda = \delta l/l = \tfrac{1}{3}\epsilon_v + (1/\sqrt{6})\epsilon_3(2\beta_3^2 - \beta_1^2 - \beta_2^2) + (1/\sqrt{2})\epsilon_2(\beta_1^2 - \beta_2^2) + 2\epsilon_{xy}\beta_1\beta_2 + 2\epsilon_{yz}\beta_2\beta_3 + 2\epsilon_{zx}\beta_3\beta_1, \quad (15)$$

where $\beta_1, \beta_2, \beta_3$ are the direction cosines of the measurement direction. The different strains are calculated for any direction of the moment, through the average values of the corresponding operators. As asserted by Alben and Callen,[17] due to the strong CEF effects, it is not possible to derive $\lambda$ as a function of the direction cosines of the moment using the classical magnetostriction coefficients $\lambda^{\alpha,0}$, $\lambda^{\gamma,2}$, and $\lambda^{\epsilon,2}$, because the modulus of the moment is anisotropic.

The calculation of the various strains has been undertaken simultaneously in the $R$Zn series with the precise determination of the $4f$ ion energy and of the magnetization for any field direction, diagonalizing the entire Hamiltonian.[18] The limits of the MF model have been checked on the magnetization curves. This model gives a better description for isothermal properties than for magnetic excitations, which seem to follow better a spin wave model. This MF defect will appear in magnetoelastic results too. For the fit in the paramagnetic state, we have verified the agreement of the calculated magnetizations with the experimental ones.[19]

The elastic constants used in the calculations have been derived from our ultrasonic measurements. We have reported in Table II the room temperature values. Their thermal variations have been taken into account as in Ref. 14 according to the results on nonmagnetic YZn by Schiltz.[20]

## III. EXPERIMENTAL METHODS

Rare-earth–zinc single crystals were obtained by direct fusion of the two components in a sealed tantalum crucible and by cooling from the melt in a Bridgman furnace; the temperature gradient was about 20 °C/cm. By this method we obtained single crystals of good size. Due to some zinc loss above 300 °C, the strains induced during the preparation of the sample could not be removed by annealing.

Spheres of about 4 mm in diameter were spark cut and used for both the magnetization measurements and the parastriction experiments which were performed with a high-sensitivity differential capacitance dilatometer.[21] The magnetic field available (3.6 kOe) with this dilatometer was not sufficient for the studies of magnetostriction in the ordered state: strain gauge experiments have been developed in the 12-kOe field provided by an electromagnet. For the latter experiments, flat disks were spark cut parallel to a high-symmetry crystallographic plane. The samples were about 10 mm in diameter and 1 mm thick. Due to the small form factor of the disks, the field is large enough to determine the spontaneous strain along the easy axes, but the forced magnetostriction can be observed only near the Curie point. Along a hard direction, the full rotation of the moment could not be achieved.

The experiments were made using electrical resistance strain gauges (micromeasurements 350 Ω). In agreement with the results found on the same type of gauges by Lee and Pourarian,[22] the gauge factor varies by about 5% between 4.2 and 300 K. As standards we used pure copper or silica samples, the thermal expansion of which was given by Hahn.[23] The absolute accuracy depends on the identity of both the two gauges and the two bindings; even for gauges manufactured at the same time, it remains at about 5%. For better accuracy, we always used two active gauges bonded along two perpendicular equivalent axes: both sets of values for the difference $\lambda_{\parallel} - \lambda_{\perp}$ between measurements parallel and perpendicular

to the field direction were in agreement better than 2%. Magnetoresistance effects were shown to be negligible at any temperature.

In the ordered state, some difficulties occur from the anisotropy of the demagnetized state. Due to the fourfold easy direction of crystal growth, the three fourfold axes are not equivalent and below the ordering point, the sample exhibits a nonzero macroscopic strain. Thus, the absolute value for the change of length $\lambda(H) = (\delta l/l)_H - (\delta l/l)_o$ can be only approached by extrapolating the isotropic values of $(\delta l/l)_o$ observed in the paramagnetic state, according to a Grüneisen-type law. But, when the sample is a single domain successively along two perpendicular equivalent axes, the difference $(\delta l/l)_{\parallel} - (\delta l/l)_{\perp}$ can be known with the preceding accuracy of 2%.

Above $T_c$, the strain gauge results have been obtained in a 10-kOe field and reduced to the values in a 1-kOe field, according to the experimental parabolic field dependence.

Complementary with the strain-gauge method, the capitance dilatometer leads to the magnetostriction with a fine accuracy ($\delta l/l \sim 10^{-8}$) in the paramagnetic state where magnetic forces are weak. The good agreement between both determinations can be checked close to the Curie point and will be discussed in Sec. IV. Thus the change of length can be observed to vary through six orders of magnitude from $10^{-2}$ to $10^{-8}$ between low and high temperatures.

This high sensivity does not permit the determination of any strain in all cases: for instance, it is difficult to obtain with accuracy $\epsilon_{xz}$ which is usually smaller than $\epsilon_3$, since any misorientation of the crystal introduces stronger parasitic strains.

## IV. DETERMINATION OF MAGNETOELASTIC CONSTANTS

We will first present the results obtained in GdZn where magnetostriction originates only from PSD interactions. Then, we shall discuss the other compounds where PSD effects either reinforce or compete with the CEF magnetoelastic coupling.

### A. GdZn

GdZn orders ferromagnetically at $T_c = 270$ K; that is the highest ordering point in all the CsCl-type compounds. Even at low temperatures, the magnetization curves are perfectly identical along the three principal axes, never showing any anisotropy larger than the experimental uncertainties. This agrees with null $B_4$ and $B_6$ CEF parameters for an $S$ state. However, we observed a tetragonal strain arising at $T_c$ (Fig. 1). As the magnetoelastic coefficient $B_1$ is null, the tetragonal strain $\epsilon_3$ originates only from the $D_1$ term. At low temperature, the spontaneous strain is $\epsilon_3 = -4.5 \times 10^{-4}$. The $D_1$ coefficient can be determined as $D_1 = -2.3 \pm 0.1$ K/atom. The MF calculated thermal variation of $\epsilon_3$ differs markedly in the 100–270 K temperature range from the experimental one. This fact may be correlated to the MF defect previously observed for the thermal variation of the spontaneous magnetization. We were not able to measure with any precision the $\epsilon_{ij}$ strains. Results for $\epsilon_v$ will be analyzed below.

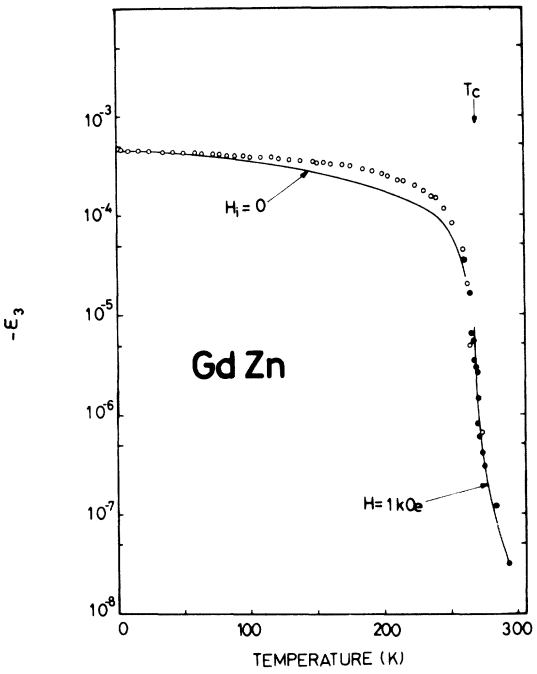


FIG. 1. Thermal variation of the spontaneous tetragonal strain $\epsilon_3 = \sqrt{\frac{3}{2}}\,\lambda[001]$ in the ordered state and of the $\epsilon_3$ strain induced by a 1-kOe field in the paramagnetic state of GdZn (○, strain-gauge data; ●, dilatometric data; full lines are calculated variations).

As the PSD coupling has been proved to contribute to the tetragonal strain in GdZn, we cannot neglect this contribution in other $R$Zn compounds. Since the coupling between $4f$ ions depends on the conduction band that is roughly the same in the series, we will keep this $D_1$ term constant. We can note [Eq. (11)] that the $D_1 \cdot \epsilon_3$ contribution modulates the Heisenberg term: it remains perfectly negligible in compounds with high-ordering points, but increases up to 2% of the isotropic exchange in ErZn.

### B. ErZn

The level scheme has been obtained in this compound by neutron spectroscopy.[4] It is defined by

$W = -0.609$ K/atom and $x = 0.16$, the four levels of the $\Gamma_8^{(3)}$ representation only being populated in all the ordered range ($T_c = 20$ K). This scheme leads to a very good fit of the three principal magnetization curves at low temperature.[4] The fit of the thermal variation for the spontaneous magnetization is good in the MF model, the CEF spacing leading to a fictious $\frac{3}{2}$ state.

In the paramagnetic state, the linear thermal expansion is of $\alpha = (9.7 \pm 0.5) \times 10^{-6}$ K$^{-1}$. Due to the anisotropy always in the same direction as the fourfold axis, only the $B_1$ coefficient can be determined in the ordered state (placing the gauges along the fourfold axes). We show in Fig. 2 the negative spontaneous strain $\epsilon_3$ below $T_c$ and the strains induced in the paramagnetic state by fields of 6 and 10 kOe. In the case of this compound alone, the calculated variations of normalized $\langle O_2^0 \rangle$ and $\langle J_z \rangle^2$ are slightly different in the ordered state. The normalized experimental $\epsilon_3$ lies between the preceeding curves, thus proving both CEF and PSD effects to contribute to this strain. We show in the inset of Fig. 2 the experimental curve together with the pseudodipolar contribution calculated with $D_1 = -2.3$ K/atom; hence we can deduce the one-ion magnetoelastic coupling coefficient $B_1$ which best fits the experimental results:

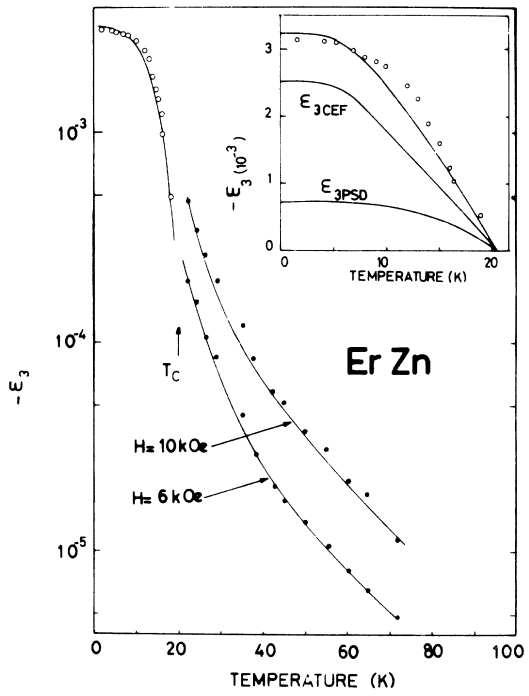


FIG. 2. Thermal variation of the spontaneous tetragonal strain $\epsilon_3 = \sqrt{\frac{3}{2}}\,\lambda[001]$ in the ordered state (○) and of the $\epsilon$ strain induced by 6- and 10-kOe fields in the paramagnetic state (●) for ErZn. Full lines are calculated curves with both CEF and PSD contributions.

$B_1 = -11.6 \pm 0.6$ K/atom.

In the paramagnetic state, with the fields available, the $\langle J_z \rangle$ values were found to be in agreement with susceptibility results and $\langle O_2^0 \rangle$ ($H$) appeared very close to $\langle J_z \rangle^2$. Both fits for $H = 6$ and 10 kOe are good, the MF model seems correct for magnetoelastic properties as well as for the magnetic properties at least in this compound. We have not been able to determine the $B_2$ coefficient from $\epsilon_{xz}$ data.

### C. DyZn

DyZn orders at 140 K, the magnetocrystalline anisotropy in the fourfold direction is always observed to be strong in the magnetization curves.[2] The negative sign of both CEF parameters in the series leads to negative values for $W$ and $x$: in all of this quadrant of the plane $(W, x)$, the energy calculated in cubic CEF and exchange fields is found to be minimized along the threefold axis. Thus both magnetoelastic and quadrupolar effects may help the fourfold axis to become the easy direction. Unfortunately, even on dilute $Dy_xY_{1-x}Zn$ compounds, neutron spectroscopy results do not allow the determination of the $(W, x)$ couple. Thus, we will first present the experimental results and then try to set boundaries on the magnetoelastic coefficients.

Placing gauges along the fourfold axes leads to the results reported for null internal field in the Fig. 3. The linear thermal expansion is $\alpha = (10.7 \pm 0.6) \times 10^{-6}$ K$^{-1}$ and the lattice behavior is in perfect agreement with the YZn results.[20] The tetragonal distortion reaches the positive value of $\epsilon_3 = (6.53 \pm 0.12) \times 10^{-3}$ at low temperature and is shown

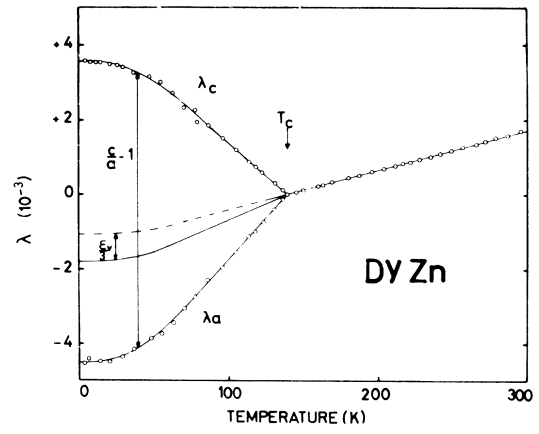


FIG. 3. Thermal variations of the changes of length, measured respectively, along the $c$ axis (parallel to the magnetization) and the $a$ axis (a fourfold axis perpendicular to the magnetization). The paramagnetic curve is extrapolated down to 0 K (dotted line) according to a Grüneisen law.

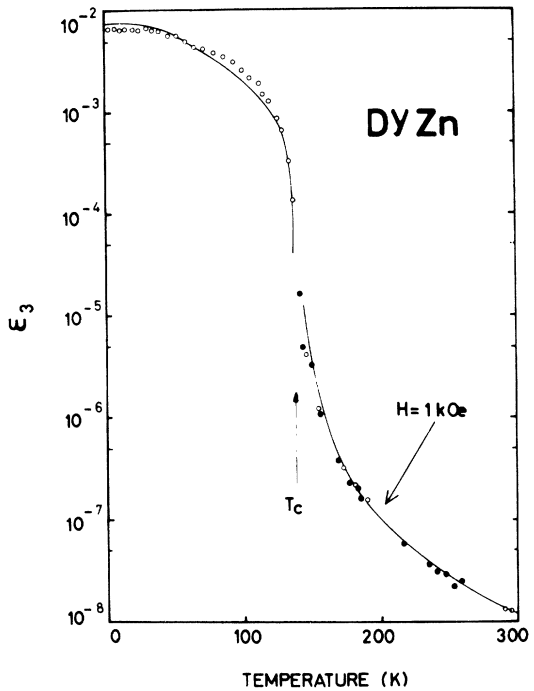


FIG. 4. Thermal variation of the spontaneous strain $\epsilon_3=\sqrt{\frac{3}{2}}\lambda[001]$ in the ordered state and of the $\epsilon_3$ strain induced by a 1-kOe field in the paramagnetic state in DyZn (○, strain-gauge data; ●, dilatometric data; full lines are calculated variations).

in Fig. 4; in the paramagnetic state, the strains are given for a field of 1 kOe. The negative volume anomaly $\epsilon_v$ will be discussed in Sec. V. As in the case of ErZn the $\epsilon_{ij}$ strain is weaker by about one order of magnitude than $\epsilon_3$; the $B_2$ coefficient, available only in the paramagnetic state, is found close to zero with large relative uncertainties.

Although the exact level scheme is unknown, we may look for the order of magnitude of $B_1$. We expect first of all that in DyZn the CEF parameters remain negative and consistent with their variations through the series: that hypothesis leads to a roughly rectangular area defined by $-0.8<W<-0.4$ and $-0.25<x<-0.10$. It is in this area, also, that the magnetization curves calculated with magnetoelastic and quadrupolar terms are found to be the best.[18] As a result of the large exchange, $\langle O_2^0\rangle$ is found to vary like the square of the magnetization. With $D_1=-2.3$ K/atom, we obtain $B_1=+16\pm2$ K/atom, $\langle O_2^0\rangle$ remaining between 70 and 90 for any possible level scheme. We have reported in the Fig. 4, the calculated curve for $W=-0.5$ K/atom, $x=-0.1$ and $B_1=+16$ K/atom. In the paramagnetic range, both magnetoelastic coefficients lead to a correct fit for an internal field of 1 kOe.

### D. TbZn

TbZn is particularly interesting because it allows a determination in the ordered state of both CEF magnetoelastic parameters $B_1$ and $B_2$, due to the change of easy direction. Indeed, the moments point along the fourfold axis from the Curie point $T_c=204$ K down to the first-order transition at $T_R=63$ K, where they rotate suddenly toward the twofold axis, that is the direction of minimum free energy at low temperature. This rotation occurs with the equality of the free energy of the twofold and fourfold phases, the different level spacings inducing a different thermal variation of the entropies and thus of the free energies.[3] This characteristic CEF effect leads, with the calculation of the moment along the three principal axes, to the level scheme defined by the couple $W=1.0\pm0.2$ K/atom, $x=-0.3\pm0.1$.

In order to determine the $B_1$ coefficient associated with the tetragonal strain, two gauges were placed along the two fourfold axes of a disk cut parallel to a fourfold plane. In the paramagnetic state, the linear thermal expansion is $\alpha=(9.2\pm0.4)\times10^{-6}$ K$^{-1}$. The extrapolation in the ordered state infers a Grüneisen-type thermal expansion (as in DyZn) and leads to a negative $\epsilon_v$ strain above $T_R$. In the same thermal range, $\epsilon_3$ increases up to $(+4.41\pm0.09)\times10^{-3}$ at $T_R$, where it vanishes suddenly (Fig. 5). In the paramagnetic

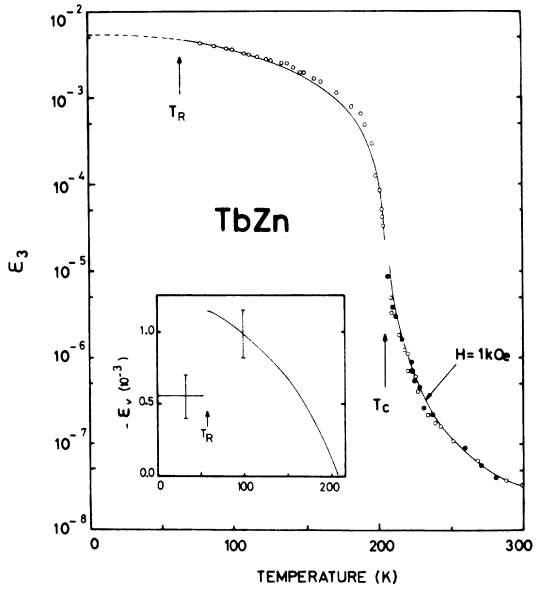


FIG. 5. Thermal variations of the spontaneous strain $\epsilon_3=\sqrt{\frac{3}{2}}\lambda[001]$ in the ordered state and of the $\epsilon_3$ strain induced by a 1-kOe field in the paramagnetic state for TbZn (○, strain-gauge data; ●, dilatometric data; full lines are calculated variations). Inset: experimental variation of the volume anomaly $\epsilon_v$.

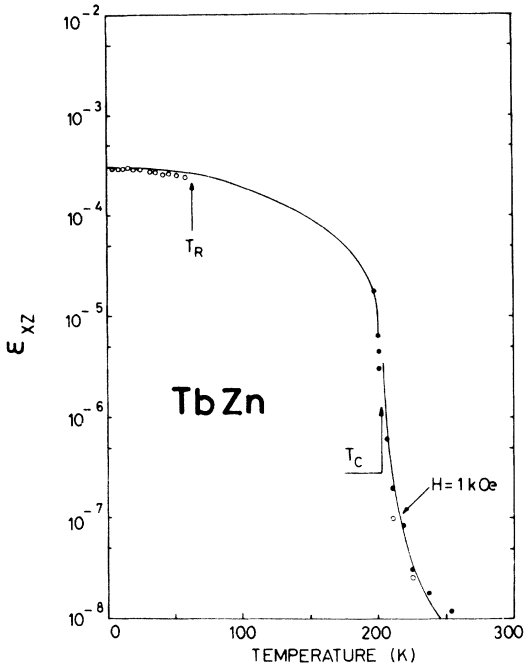


FIG. 6. Thermal variations of the spontaneous strain $\epsilon_{xz}$ ($T<T_R$) and of the $\epsilon_{xz}$ strain induced by a 1-kOe field in the paramagnetic range for TbZn (○, strain-gauge data; ●, dilatometric data; full lines are calculated variations).

range strain gauges and dilatometer give the same results for a field of 1 kOe. Below $T_R$, the applied field is too weak to rotate the moments toward the hard fourfold axis and $\epsilon_3$ cannot be measured. Results obtained when the field is applied along the easy twofold axis will be discussed in addition to $\epsilon_v$ in Sec. V.

Taking into account the PSD contribution, the calculation for the preceding levels scheme gives a satisfactory agreement with the experimental $\epsilon_3$ using a magnetoelastic coefficient $B_1=+15\pm1$ K/atom. Uncertainties on the scheme do not have much influence on the $\langle O_2^0\rangle$ values, the $4f$ wave function being largely purified of CEF effects by the strong exchange. In the paramagnetic state, the moment values used in the fit are in agreement with magnetic susceptibility measurements and $\epsilon_3$ calculated values agree with experimental results.

In order to determine the spontaneous strain $\epsilon_{xz}$ below $T_R$ and above $T_c$, two gauges were placed along the [101] and [$\bar{1}$01] axes of the same disk. The field was applied successively in both directions and the half difference of the measurements leads to

$$\tfrac{1}{2}(\lambda_{[101]}-\lambda_{[\bar{1}01]})=\epsilon_{xz}\,. \tag{16}$$

The temperature dependence of $\epsilon_{xz}$ is reported in Fig. 6. The positive spontaneous strain is one order of magnitude weaker than $\epsilon_3$. As the $D_2$ coefficient was not obtained in GdZn, we shall fit $\epsilon_{xz}$ only in terms of the one ion $B_2$ coefficient. The calculated values for $\langle P_{xz}\rangle$ in the same level spacing leads to $B_2=+11.6\pm0.8$ K/atom at 4.2 K. Although we observe a discrepancy when approaching $T_R$, this $B_2$ coefficient provides a good fit of the paramagnetic results. Note that the half-sum of both measurements along [101] and [$\bar{1}$01] can be written

$$\tfrac{1}{2}(\lambda_{[101]}+\lambda_{[\bar{1}01]})=\tfrac{1}{3}\epsilon_v+\tfrac{1}{2}(\epsilon_3/\sqrt{6}+\epsilon_2/\sqrt{2})\,. \tag{17}$$

Its thermal variation will be discussed in Sec. V.

### E. HoZn

In this compound, which orders at $T_c=74$ K, there is, also, a change of easy direction between the twofold axis stable below $T_R=23$ K and the threefold one above. This first order transition has been observed by specific heat[3] and magnetization experiments.[2] In particular, the shift of $T_R$ under magnetic fields is readily apparent on the magnetization curves relative to the [110] and [111] axes.

The level scheme defined by $W=0.36$ K and $x=0.08$ has been determined by neutron spectroscopy.[4] While the fourfold axis is always a very hard direction, the other two principal axes are

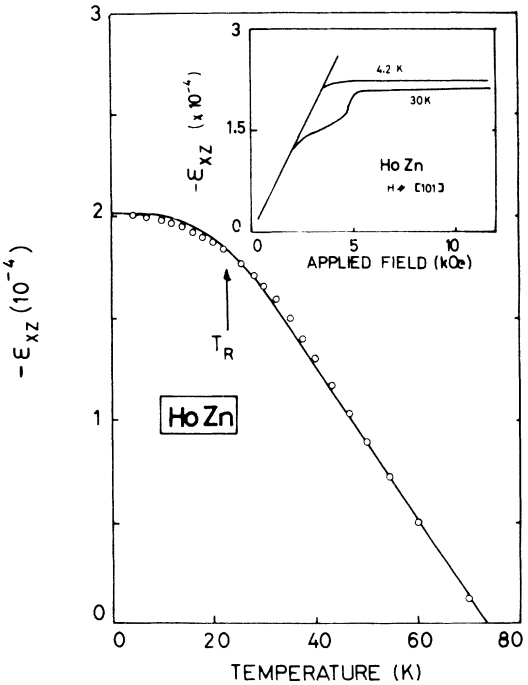


FIG. 7. Thermal variations of the spontaneous strain $\epsilon_{xz}$ for HoZn. Inset: field dependence of the strain $\epsilon_{xz}$ at 4.2 (twofold easy axis) and at 30 K (threefold easy axis).

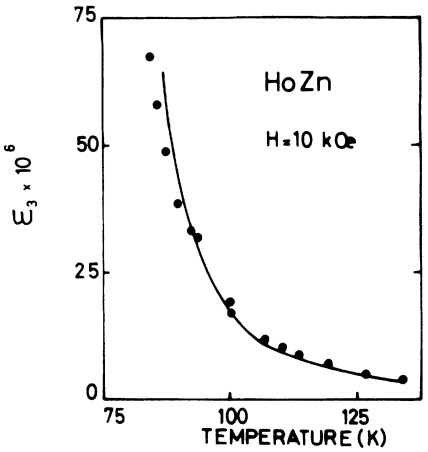


FIG. 8. Thermal variation of the $\epsilon_3$ strain induced by a 10-kOe field in the paramagnetic state of HoZn.

found to be very close in energy. Thus an internal field of 5 kOe is large enough to align the moments along the twofold axis above $T_R$. On all the samples studied we have found a linear thermal expansion of $\alpha = (11.2 \pm 0.7) \times 10^{-6}$ K$^{-1}$ in the paramagnetic state.

With gauges parallel to the twofold axes, Eq. (16) leads to a gap in $\epsilon_{xz}$ (inset of Fig. 7) above $T_R$, as in the corresponding magnetization curves.[2] That is explained by the variation of $\langle P_{xz} \rangle$ with the rotation of the moment from the threefold easy axis to the twofold field direction. Starting with the level scheme and neglecting the PSD contribution ($D_2 \simeq 0$), the thermal variation of $\epsilon_{xz}$ gives a magnetoelastic coefficient $B_2 = -6.4 \pm 0.4$ K/atom. As in TbZn, Eq. (17) will contribute to further study of $\epsilon_v$ after the determination of the tetragonal $B_1$ coefficient.

The $\epsilon_3$ strain has been measured in the paramagnetic state, with gauges and field along fourfold axes. Using the moment values obtained along fourfold axes above $T_c$ in order to calculate the thermal variations of $\langle O_2^0 \rangle$ and of the PSD term, the fit leads to a good agreement with experiments as it can be seen in the Fig. 8 for a field of 10 kOe. Both observed and calculated field variations of $\epsilon_3$ follow closely an $H^2$ law in all the studied range. The $B_1$ coefficient is found to be $B_1 = +(8.4 \pm 0.4)$ K/atom. The change of length when the field is applied along a twofold axis in the ordered state will be analyzed in Sec. V.

## V. VOLUME MAGNETOSTRICTION

We will now discuss the fully symmetrical mode $\epsilon_v$. The magnetoelastic Hamiltonian consists of two contributions. First the exchange terms of the general Hamiltonian can be modulated by $\epsilon_v$:

$$\mathcal{H}^{II}_{\epsilon_v} = -\epsilon_v \frac{\partial \mathcal{J}}{\partial \epsilon_v} (\langle J_z \rangle J_z + \cdots) - \epsilon_v \left( \frac{\partial K_1}{\partial \epsilon_v} (\langle O_2^0 \rangle O_2^0 + 3 \langle O_2^2 \rangle O_2^2) + \frac{\partial K_2}{\partial \epsilon_v} (\langle P_{xz} \rangle P_{xz} + \cdots) \right) . \quad (18)$$

$\mathcal{J}$ is the Heisenberg exchange integral and $K_1$ and $K_2$ the quadrupolar exchange constants.

The modulation of the one-ion CEF terms leads to

$$\mathcal{H}^{I}_{\epsilon_v} = -\frac{\partial B_4}{\partial \epsilon_v} \epsilon_v (O_4^0 - 5O_4^4) - \frac{\partial B_6}{\partial \epsilon_v} \epsilon_v (O_6^0 - 21O_6^4) , \quad (19)$$

which contributes to the anomalous thermal expansion at all temperatures, as first observed by Ott and Lüthi on TmSb.[24] At the ordering point, the thermal average value of fourth- and sixth-order operators is modified by the exchange field. Then $\epsilon_v$ is given in the ordered state by the following expression limited to the terms linear in strains:

$$\epsilon_v(T) \sim \frac{\partial \mathcal{J}}{\partial \epsilon_v} (\langle J_z \rangle^2 + \cdots) + \frac{\partial K_1}{\partial \epsilon_v} (\langle O_2^0 \rangle^2 + 3 \langle O_2^2 \rangle^2) + \frac{\partial K_2}{\partial \epsilon_v} (\langle P_{xz} \rangle^2 + \cdots) + \frac{\partial B_4}{\partial \epsilon_v} (\langle O_4 \rangle_{H_{ex}} - \langle O_4 \rangle_{H_{ex}=0}) + \frac{\partial B_6}{\partial \epsilon_v} (\langle O_6 \rangle_{H_{ex}} - \langle O_6 \rangle_{H_{ex}=0}) + \cdots . \quad (20)$$

Due to the complexity of the problem, $\epsilon_v$ will be only treated qualitatively.

In order to obtain $\epsilon_v$, we have to use combinations of the different strains such as $\lambda_{[001]} + 2\lambda_{[100]}$ (gauges and moments parallel to fourfold axes), $\lambda_{[101]} + \lambda_{[\bar{1}01]}$ [gauges and moments along twofold axes, see Eq. (17)]. These changes of length $\lambda_{[ijk]}$ have to be determined by difference from the unstrained lattice behavior extrapolated from the paramagnetic state. Our Grüneisen-type law agrees with the thermal-lattice behavior of YZn,[20] but the cumulated uncertainties on $\epsilon_v$ can reach 20%.

In the ordered state of DyZn, $\epsilon_v$ has been obtained from the results of Fig. 3 and reported in Fig. 9. $\epsilon_v$ is negative, reaching $(-2.2 \pm 0.2) \times 10^{-3}$ at 4.2 K and follows roughly a thermal $\langle J_z \rangle^2$ law. This is consistent with the negative forced magnetostriction above $T_c$, which also varies as $\langle J_z \rangle^2$. If we define a total magnetoelastic coefficient

$$\mathfrak{D}_o = \epsilon_v C_B / \langle J_z \rangle^2 , \quad (21)$$

we obtain for DyZn a negative value $\mathfrak{D}_o = -10 \pm 1$ K/atom. In ErZn we observed $\epsilon_v$ and its field derivative to be both negative, but the measurements were too inaccurate to obtain a value for $\mathfrak{D}_o$.

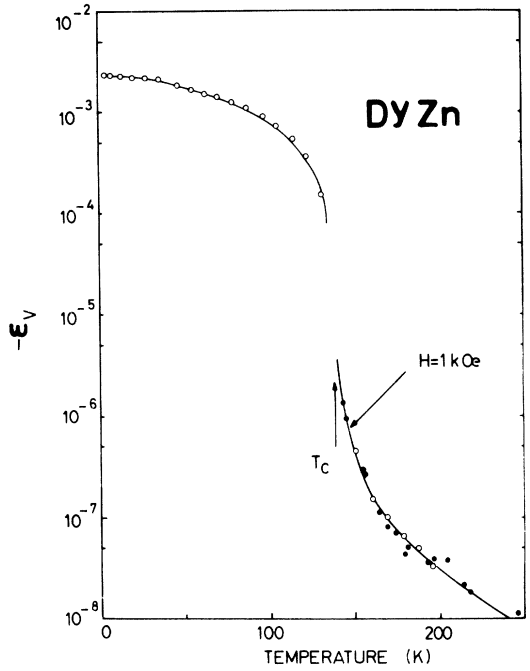


FIG. 9. Thermal variations of the spontaneous volume change $\epsilon_v$ in the ordered state and of the $\epsilon_v$ strain induced by a 1-kOe field in the paramagnetic state (○, strain-gauge data; ●, dilatometric data; full lines are calculated variations).

In the paramagnetic state of HoZn we observed the negative sign for the field derivative when measuring the $\epsilon_3$ strain (gauges and moments parallel to fourfold axes). In the ordered state with the moments always remaining along the twofold axes, the change of length is

$$\lambda_{[001]} = \tfrac{1}{3}\epsilon_v + (2/\sqrt{6})\epsilon_3 . \tag{22}$$

Calculations allow us to verify that both Eqs. (17) and (22) are identical for a moment along a twofold axis. Both determinations are reported in Fig. 10. After subtracting the calculated $\epsilon_3$ contribution, $\epsilon_v$ is found to be about $(-2.2 \pm 0.3) \times 10^{-3}$ at 4.2 K, and varying like the square of magnetization ($\mathfrak{D}_0 = -9 \pm 2$ K/atom).

In TbZn, $\epsilon_v$ has been studied with both gauge orientations. Between $T_c$ and $T_R$, we observed the same behavior as previously in HoZn with $\mathfrak{D}_0 \simeq -8 \pm 2$ K/atom (Inset of Fig. 5). But at $T_R$ there appears a marked step, $\epsilon_v$ remaining negative. As the magnetization has been observed to be only 2% larger in the twofold axis, that is not enough to explain this step, without taking into account the different average values of CEF operators on both sides of $T_R$. Note that, in this particular case of TbZn, the $\partial B_4/\partial \epsilon_v$ crystal effect can contribute. This fact was not observed in HoZn, because we could keep the moments along the [101] hard direction with a 5-kOe field above $T_R$.

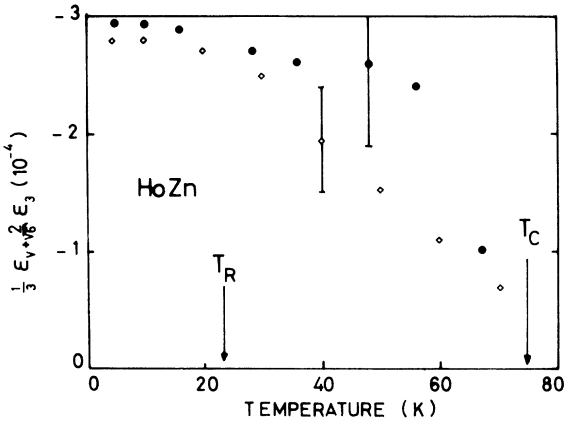


FIG. 10. Thermal variations of the change of length $\frac{1}{3}\epsilon_v + (2/\sqrt{6})\epsilon_3$ (●, gauges parallel to [101]; ◇, gauges parallel to [001]).

In GdZn, the paramagnetic range investigated is too small to expect a determination of $\epsilon_v$ from an extrapolation in the ordered state. But close to $T_c$, we have found $\epsilon_v$ to be positive as well as its field derivative. This is opposite to the results for the other compounds. In GdZn, $\epsilon_v$ is only due to the variation of exchange with the lattice parameter and can be written

$$\epsilon_v = (D_0/C_B)(\langle J_z \rangle^2 + \cdots) , \tag{23}$$

$D_0$ being the corresponding magnetoelastic coefficient. The positive value of $D_0$ is confirmed by the analysis of isotropic pressure experiments by Hiraoka.[25] This author observed a negative dependence of the ordering point $T_c$ with the pressure. According to the Bean and Rodbell theory,[26] we can deduce from his results a positive value $D_0 = +7$ K/atom.

## VI. DISCUSSION

We have collected all the results obtained through the series in Table II.

### A. Lattice thermal expansion

The linear thermal-expansion coefficient in the paramagnetic state was found to vary from (9.2) $\times 10^{-6}$ to $(11.0) \times 10^{-6}$ K$^{-1}$ through the series, but it is difficult to say whether this variation is to be associated with a lattice effect rather than with gauge defects. Our values agree with that given for YZn by Schiltz *et al.*,[20] who found $\alpha = (11 \pm 1) \times 10^{-6}$ K$^{-1}$, constant between 80 and 300 K.

### B. Anomalous volume expansion

GdZn exhibits a pure exchange striction. In all the other compounds, exchange and CEF effects

TABLE II. Background elastic constants at room temperature, linear thermal expansion ($T > 70$ K), spontaneous strains at 4.2 K ($\sqrt{\frac{3}{2}}\epsilon_3 = c/a - 1$), magnetoelastic coefficients and Stevens coefficients (N.M. = not measured).

| $R$Zn | GdZn | TbZn | DyZn | HoZn | ErZn |
|---|---|---|---|---|---|
| $C_{11}-C_{12}$ $10^5$ K/atom | 1.07 | 1.09 | 1.20 | 1.41 | 1.74 |
| $C_{44}$ $10^5$ K/atom | 1.25 | 1.28 | 1.43 | 1.53 | 1.65 |
| $C_B$ $10^5$ K/atom | 1.99 | 1.97 | 2.03 | 1.83 | 2.28 |
| $\alpha$ $10^{-6}$ K$^{-1}$ | N.M. | 9.2±0.4 | 10.7±0.6 | 11.0±0.7 | 9.7±0.5 |
| $\epsilon_v$ ($10^{-3}$) (4.2 K) | >0 | ~−1.3 (63 K) ~−0.5 (4.2 K) | −2.2±0.2 | −2.3±0.3 | <0 |
| $\epsilon_3$ ($10^{-3}$) (4.2 K) | −0.45 | +4.41 (63 K) | +6.53 | N.M. | −3.10 |
| $\epsilon_{xz}$ ($10^{-3}$) (4.2 K) | N.M. | +0.3 | N.M. | −0.2 | N.M. |
| $B_1$ (K/atom) | 0 | +15±1 | +16±2 | +8.4±0.4 | −11.6±0.6 |
| $B_2$ (K/atom) PSD neglected | | +11.6±0.8 | | −6.4±0.4 | |
| $\alpha_J$ ($10^{-2}$) | 0 | −1.01 | −0.635 | −0.222 | +0.254 |

both contribute to the anomalous volume change $\epsilon_v$, but the CEF contribution appears to be three times larger than exchange striction—and opposite in sign. This explains, for instance, the unusual step in the curve $\epsilon_v(T)$ observed with TbZn for $T = T_R$, a typical CEF effect.

### C. $B_1$ magnetoelastic coefficient

$B_1$ is derived from the experimental $\epsilon_3$ strain, after having subtracted the two-ion ($D_1$) contribution. In the present case of a simple cubic lattice, the $B_1$ magnetoelastic coefficient is proportional to the strain derivative of the second-order CEF parameter $\alpha_J\langle r^2\rangle A_2$. The contribution of the surroundings $A_2$ is null only in the cubic phase, but its strain derivative is not null and may be taken as constant through the series. So we can expect $B_1$ to vary throughout the series proportionally to $\alpha_J\langle r^2\rangle$, where $\alpha_J$ (the Stevens coefficient) and $\langle r^2\rangle$ are relative to the $4f$ shell and independent of the strains in the first approximation.

This law is well verified in Fig. 11 and confirmed in the case of TmZn ($B_1 = -25 \pm 3$ K/atom) that we have recently investigated.[27] Ultrasonic determinations for ErZn and TmZn are also reported in the Fig. 11, and will be discussed later. Moreover, we can note that the strong tetragonal strains observed in antiferromagnetic $R$Zn ($c/a - 1 = +1.4\%$ with PrZn,[28] +1.6% with[29] CeZn) are consistent with the large negative values for $\alpha_J\langle r^2\rangle$.

The good agreement between $-\alpha_J\langle r^2\rangle$ and $B_1$ in all the series justifies *a posteriori* our assumption that the PSD $D_1$ contribution, which depends chiefly on the band structure, is roughly constant through the series.

### D. $B_2$ magnetoelastic coefficient

As explained in Sec. III, it is usually difficult to determine $\epsilon_{xz}$. The evaluation of the PSD $D_2$ coef-

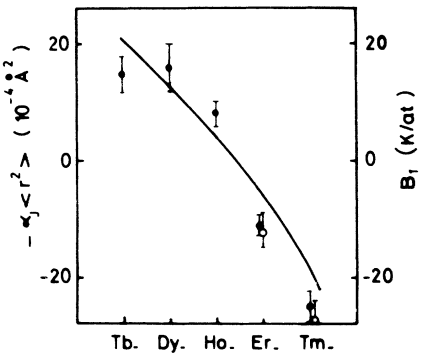


FIG. 11. Variations of the $B_1$ magnetoelastic coefficient and of the $\alpha_J\langle r^2\rangle$ term throughout the $R$Zn series. The error's bars do not take into account any uncertainties on the $D_1$ PSD term [full line, $\alpha_J\langle r^2\rangle$; $B_1$, ●, this study; ○, from ultrasonic data (Refs. 14 and 30)].

ficient was not possible from our $\epsilon_{xz}$ measurements on GdZn and we could obtain $\epsilon_{xz}$ only in the ordered state of TbZn and HoZn. If the $D_2$ contribution is neglected, both $B_2$ values do not follow the $\alpha_J\langle r^2\rangle$ law; in both compounds, the agreement requires as for $D_1$ a negative value of $D_2$. A similar negative $D_2$ value is necessary to explain the null $\epsilon_{xz}$ strain observed in the paramagnetic range of DyZn. Thus it appears that for this $\epsilon_{xz}$ strain too, the PSD contribution takes an important part in the magnetostriction.

### E. Comparison with dynamic determination

Both magnetoelastic coefficients $B_1$ and $B_2$ can be approached by ultrasonic experiments. Calculations have been developed for the paramagnetic state in the recent past for the thermal variation of elastic constants in presence of CEF effects.[11] For instance, the $C_{11}-C_{12}$ mode is given by expression (3) in Ref. 14:

$$\frac{C_{11}-C_{12}}{(C_{11}-C_{12})_o}=\frac{1+(g_2^2+g')\chi_s}{1+g'\chi_s},$$

where $\chi_s$ is the strain susceptibility depending on the level scheme, the magnetoelastic coefficient $g_2$ is proportional to our $B_1$ and $g'$ corresponds to the quadrupolar exchange coupling $K_1$ of expression (2). Thus in ultrasonic experiments, the $B_1^2$ term has to be isolated from $K_1$; besides, one cannot obtain the sign of $B_1$. This method is suitable for compounds with low ordering point, like ErZn and TmZn: curve fitting for the $C_{11}-C_{12}$ mode leads to $g_2^2=0.8\pm0.1$ mK, (i.e., $|B_1|=12\pm1$ K/atom) in[30] ErZn and to $g_2^2=8.9\pm0.5$ mK, (i.e., $|B_1|=30\pm2$ K/atom) in TmZn.[14] We have reported in the Fig. 11 these values with the negative sign observed by magnetostriction experiments. The good agreement in both experimental determinations comforts us about the hypothesis of a constant $D_1$ magnetoelastic contribution and, besides, indicates the existence of the quadrupolar coupling. The fact that no softening appears on the $C_{44}$ mode confirms the smaller role of $B_2$ in magnetostriction.

### F. Tentative analysis of magnetoelastic coupling

The first attempt is usually to compare the magnetoelastic coefficients with point charge model predictions. According to the Hutchings formalism,[31] the CEF magnetoelastic term $B_1$ can be written

$$B_1=(e^2/a^3)[3q_R-(64/9\sqrt{3})q_{Zn}]\sqrt{\tfrac{3}{2}}\,\alpha_J\langle r^2\rangle,$$

when taking into account the eight zinc and six rare-earth first neighbors. Assuming $q_R=+3$ and $q_{Zn}=+2$ leads to $B_1\simeq+2$ K/atom, that can be modified by the further neighbors contributions. As in our intermetallics the CEF parameters have been proved not to follow such a model, but been related mainly to the conduction band, any agreement on $B_1$ would be accidental.

Since the CEF parameters are stated by the electronic structure in the close surroundings of the $4f$ ion, understanding would be facilitated by a good knowledge of the band. But the hard theoretical problem of the magnetoelastic coefficients would necessitate calculating first both the direct and exchange coulombic contributions to CEF parameters, before studying their strain modification. A first rough idea is that a tetragonal strain splits the degeneracy of the $e_g$ band lying close to the Fermi level and thus selects particular orbitals. This mechanism occurs simultaneously with $4f$ ordering through the $4f$ shell-band coupling but the interactions through the conduction band between intrinsic $4f$ quadrupoles, observed without magnetic ordering in TmZn,[27] may proceed from the same origin. The PSD magnetoelastic coupling, too, may be expected to be interpreted in the band model.


[1] A. Iandelli and A. Palenzona, J. Less Common Metals 9, 61 (1965); K. Kanematsu, G. T. Alfieri, and E. Banks, J. Phys. Soc. Jpn. 26, 244 (1969).

[2] P. Morin and J. Pierre, Solid State Commun. 13, 537 (1973); Phys. Status Solidi A 17, 479 (1973); R. Aleonard, P. Morin, and J. Pierre, Colloque International Centre National de Recherche Scientifique, "Physics in High Magnetic Fields," Grenoble, 1974 (unpublished).

[3] P. Morin and A. De Combarieu, Solid State Commun. 17, 975 (1975); P. Morin, J. Pierre, and J. Chaussy, Phys. Status Solidi A 24, 425 (1974).

[4] P. Morin, J. Pierre, J. Rossat-Mignod, K. Knorr, and W. Drexel, Phys. Rev. B 9, 4932 (1974); P. Morin, J. Pierre, D. Schmitt, and W. Drexel, J. Phys. (Paris) 37, 611 (1976); D. Schmitt, P. Morin, and J. Pierre, Phys. Rev. B 15, 1698 (1977).

[5] P. Morin and J. Pierre, Phys. Status Solidi A 21, 161 (1974). The results reported have been obtained by x-ray experiments on splash-cooled polycrystalline sheets as the compounds are too soft to give narrow lines from powders. But the induced texture led to some errors about the sign of spontaneous strains.

[6] G. Williams and L. Hirst, Phys. Rev. 185, 407 (1969).

[7] H. C. Chow, Phys. Rev. B 7, 3404 (1973).

[8] J. Høg and P. Touborg, Phys. Rev. B 9, 2920 (1974); Phys. Rev. Lett. 33, 775 (1974).

[9] See, for instance, M. Belakhovsky, J. Pierre, and D. K. Ray, J. Phys. F 5, 2274 (1975); M. Belakhovsky and D. K. Ray, Phys. Rev. B 12, 3956 (1975).

[10]K. R. Lea, M. J. M. Leask, and W. P. Wolf, J. Phys. Chem. Solids 23, 1381 (1962).
[11]G. A. Gehring and K. A. Gehring, Rept. Prog. Phys. 38, 1 (1975).
[12]P. Levy, J. Phys. C 6, 3545 (1973).
[13]B. Lüthi, M. E. Mullen, K. Andres, E. Bucher, and J. P. Maita, Phys. Rev. B 8, 2639 (1973).
[14]P. Morin, A. Waintal, and B. Lüthi, Phys. Rev. B 14, 2972 (1976).
[15]E. Callen and H. B. Callen, Phys. Rev. 139, A455 (1965).
[16]B. Lüthi, P. S. Wang, Y. H. Wong, H. R. Ott, and E. Bucher, Proceedings of the Second International Conference on Crystalline Electric Field Effects in Metals and Alloys, Zurich, 1976 (Pergamon, New York, to be published).
[17]R. Alben and E. Callen, Phys. Rev. 186, 522 (1969).
[18]D. Schmitt and P. Morin (unpublished).
[19]P. Morin, thesis (University of Grenoble, Centre National de la Recherche Scientifique, A.O. 9323, 1975) (unpublished).
[20]R. J. Schiltz, Jr., T. S. Prevender, and J. F. Smith, J. Appl. Phys. 42, 4680 (1971).
[21]E. de Tremolet de Lacheisserie, Rev. Phys. Appl. 10, 169 (1975).
[22]E. W. Lee and F. Pourarian, Phys. Status Solidi A 33, 483 (1976); 34, 383 (1976).
[23]T. A. Hahn and R. K. Kirby, AIP Conf. Proc. 3, 13 (1971); T. A. Hahn, J. Appl. Phys. 41, 5096 (1970).
[24]H. R. Ott and B. Lüthi, Phys. Rev. Lett. 36, 600 (1976).
[25]T. Hiraoka, J. Phys. Soc. Jpn. 37, 1238 (1974).
[26]C. P. Bean and D. S. Rodbell, Phys. Rev. 126, 104 (1962).
[27]P. Morin, J. Rouchy, and D. Schmitt (unpublished).
[28]P. Morin and J. Pierre, Phys. Status Solidi A 30, 549 (1975).
[29]P. Morin and D. Schmitt (unpublished).
[30]P. Morin, A. Waintal, and B. Lüthi, Proceedings of the Twelfth Rare Earth Research Conference, Vail, Colorado, 1976 (unpublished).
[31]M. T. Hutchings, Solid State Phys. 16, 277 (1964).